

THE FLORIDA STATE UNIVERSITY  
COLLEGE OF ARTS AND SCIENCES

PRINCIPAL PATTERNS OF INTERANNUAL REGIONAL AUSTRALIAN  
RAINFALL VARIABILITY AND THEIR RELATIONSHIP TO INDIAN  
OCEAN EVAPORATION

By

KENNETH W. EKERS

A Thesis submitted to the  
Department of Meteorology  
in partial fulfillment of the  
requirements for the degree of  
Master of Science

Degree Awarded:  
Spring Semester, 1995

Degree Awarded:  
Spring Semester, 1995

## APPENDIX B

### ROTATION OF EOFs

Patterns of spatially unrotated eigenvectors are shown to be predictable (Buell, 1975); e.g. EOF1 of any given precipitation data set displays the majority of the explained variance with large values, all of which are the same sign, while each consecutive significant EOF displays 'drumhead' modes (oscillating patterns of positive and negative values). Unrotated eigenvectors also show conflicting localized patterns in a full domain as compared with subdomains. Richman (1986) discusses these and other characteristics which question the reliability of analyzed unrotated eigenvectors.

The rotation of eigenvectors offers potential advantages when examining individual modes (Cliff and Hamburger (1967), Horel (1981), and Richman, 1986). The rotation of eigenvectors attempts to correct the unrotated EOF solutions by identifying coherent modes in each significant spatial field. These individual modes of variation often relate to known physical phenomena. The concept behind these modes is known as simple structure (Kaiser 1958; Horel 1981; Richman 1986). Simple structure aids in discovering an underlying order in the data set. Rotation of eigenvectors has been shown to improve representation of meteorological variables such as precipitation and SSTs (Walsh et al., 1982; Nicholls, 1989; Elsner and Tsonis, 1992; Drosowsky, 1993a). Thus, this study considers the use of rotation important.

Drowsdowsky (1993a) points out that two intricate obstacles arise in considering the use of rotation important.

Drowsdowsky (1993a) points out that two intricate obstacles arise in the rotation of eigenvectors. First, the significant eigenvectors (number of

eigenvectors retained for rotation) are not determined by any acceptable criterion. The loadings are dependent on the number of significant eigenvectors. Second there exists several possible types of rotation (e.g. orthogonal rotations, oblique rotations and Procrustes target rotations). Richman (1986) mentions 19 orthogonal and oblique rotations; thus selecting a method can be difficult.

To solve the first problem, the utilization of a Monte Carlo simulation method, Rule N, as presented by Preisendorfer (1988) determines the number of significant eigenvectors. By generating random sequences, a statistical limit for significant eigenvalues based on their percentage of variance of the data can be determined. Utilization of a 95% confidence level determines which eigenvalues are significant and thus how many eigenvectors are rotated.

This study addresses the second problem through a comparison of rotated EOFs. A detailed description of this comparison is found in section 3.2 of this study. The conclusion is to use the varimax orthogonal rotation.

This study linearly transforms the set of eigenvectors,  $V$ , to a set of spatially uncorrelated orthogonal components,  $V^*$ . The transformation procedure is the normalized orthogonal varimax rotation. This method uses normalized square loadings of the significant unrotated eigenvectors to solve for the maximum variance,  $VAR$ , i.e. maximize

$$VAR = \sum_{j=1}^{S^*} \left[ S \sum_{i=1}^S (d_{i,j}^2/n_i^2)^2 - \left[ \sum_{i=1}^S d_{i,j}^2/n_i^2 \right]^2 / S^2 \right]$$

where  $d_{i,j}$  are the loadings,  $S^*$  is the number of significant eigenvectors,  $S$

where  $d_{i,j}$  are the loadings,  $S^*$  is the number of significant eigenvectors,  $S$  is the number of stations and  $n_i$  is the communality of the  $i$ th station. The

varimax criterion requires orthogonal rotation of the significant eigenvector pairs until *VAR* is maximized. These loadings make up the transformed set of rotated eigenvectors.

## REFERENCES

- Allan, R.J., 1983: Monsoon and teleconnection variability over Australasia during the southern hemisphere summers of 1973-77. *Mon. Wea. Rev.*, **111**, 113-142.
- Allan, R.J., 1985: The Australasian summer monsoon, teleconnections, and flooding in the Lake Eyre Basin. Royal Geographical Society of Australasia. *South Australian Geographical Review Papers*, **2**, 47 pp.
- Allan, R.J., 1988: Climatic conditions during the 1973-1976 Lake Eyre flooding/filling. In "The great filling of Lake Eyre in 1974". Royal Geographical Society of Australasia, South Australian Branch.
- Allan, R.J., J.A. Bye and P. Hutton, 1986: The 1984 filling of Lake Eyre South. *Trans R. Soc. S. Aust.*, **110**(2), 81-87.
- Allan, R.J. and M.R. Haylock, 1993: Circulation features associated with the winter rainfall decreases in southwestern Australia. *J. Climate*, **6**, 1356-1367.
- Angell, J.K., 1981: Comparison of variations in atmospheric quantities with sea-surface temperature variations in the equatorial eastern Pacific. *Mon. Wea. Rev.*, **109**, 230-243.
- Baines, P.G., 1990: What's interesting and different about Australian meteorology?. *Aust. Met. Mag.*, **38**, 123-141.
- Barnett, T., 1991: The interaction of multiple time scales in the tropical climate system. *J. Climate*, **4**, 269-285.
- Buell, C.E., 1975: The topography of empirical orthogonal functions. *Preprints Fourth Conf. on Prob. and Stats, in Atmos. Sci.*, Tallahassee, Fl, Amer. Meteor. Soc. 188.
- Bureau of Meteorology, 1975: *Map of Seasonal Rainfall Zones*. Bur. Met. Australia.
- Burroughs, W.J., 1992: *Weather cycles: Real or imaginary?*. Cambridge University Press., 201 pp.
- Burroughs, W.J., 1992: *Weather cycles: Real or imaginary?*. Cambridge University Press., 201 pp.
- Cardone, V.J., J.G. Greenwood and M.A. Cane, 1990: On trends in historical marine wind data. *J. Climate*, **3**, 113-127.

- Cliff, N. and C.D. Hamburger, 1967: A study of sampling errors in factor analysis by means of artificial experiments. *Psych. Bull.*, **68**, 430.
- Conrad, V., 1941: The variability of precipitation. *Mon. Wea. Rev.*, **69**, 5-11.
- Drosowsky, W., 1993a: An analysis of Australian seasonal rainfall anomalies:1950-1987.I: Spatial patterns. *Int. J. Climatol.*, **13**, 1-30.
- Drosowsky, W., 1993b: An analysis of Australian seasonal rainfall anomalies:1950-1987.I: Temporal variability and teleconnection patterns. *Int. J. Climatol.*, **13**, 111-149.
- Drosowsky, W., 1993c: Potential predictability of winter rainfall over southern and eastern Australia using Indian Ocean sea-surface temperature anomalies. *Aust. Met. Mag.*, **42**, 1-6.
- Elsner, J.B. and A.A. Tsonis, 1992: A note on the spatial structure of the covariability of observed northern hemisphere surface air temperatures. *Pageoph*, **137**, 133-146.
- Horel, J.D., 1981: A rotated principal component analysis of the interannual variability of the northern hemisphere 500 mb height field., *Mon. Wea. Rev.*, **109**, 2080-2092.
- Jolliffe, I.T., 1986: *Principal Component Analysis*. Springer-Verlag New York Inc., 271 pp.
- Jones, C.S., D.M. Legler and J.J. O'Brien, 1994: Variability of surface fluxes over the Indian Ocean; 1960-1989. Accepted *The Atmos. Ocean Sys.*
- Kaiser, H.F., 1958: The varimax criterion for analytic rotation in factor analysis. *Psychometrika*, **23**, 187-200.
- Lavery, M.B., A.P. Kariko and N. Nicholls, 1992: A historical rainfall data set for Australia., *Aust. Met. Mag.*, **40**, 33-39.
- Lough, J.M., 1993: Variations of some seasonal rainfall characteristics in Queensland, Australia: 1921-1987. *Int. J. Climatol.*, **13**, 391-409.
- McBride, J.L. and N. Nicholls, 1983: Seasonal relationships between Australian rainfall and the Southern Oscillation. *Mon. Wea. Rev.*, **111**, 1998-2004.
- Miles, K.F., D.M. Legler and J.J. O'Brien, 1993: Variability of five day wind fields over the Indian Ocean using ship and SASS Data. To appear in *The Atmos. Ocean Sys.*
- Miles, K.F., D.M. Legler and J.J. O'Brien, 1993: Variability of five day wind fields over the Indian Ocean using ship and SASS Data. To appear in *The Atmos.-Ocean Sys.*



- Nicholls, N., 1988: El Niño-Southern Oscillation and rainfall variability. *J. Climate*, **1**, 418-421.
- Nicholls, N., 1989: Sea-surface temperatures and Australian winter rainfall. *J. Climate*, **2**, 965-973.
- Nicholls, N., 1992: Historical El Niño/Southern Oscillation variability in the Australasian region. In Diaz, H.F. and V. Markgraf (eds.), *El Niño: Historical and Paleoclimatic Aspects of the Southern Oscillation*. Cambridge University Press, 151-173.
- Nicholls, N. and A. Kariko, 1993: East Australian rainfall events: Interannual variations, trends, and relationships with the Southern Oscillation. *J. Climate*, **6**, 1141-1152.
- Nicholls, N. and B.M. Lavery, 1992: Australian rainfall trends during the twentieth century. *Int. J. Climatol.*, **12**, 153-163.
- Nicholls, N. and F. Woodcock, 1981: Verification of an empirical long range weather forecasting technique. *Quart. J. Roy. Meteor. Soc.*, **107**, 973-976.
- Nicholls, N. and K. Wong, 1990: Dependence of rainfall variability on mean rainfall, latitude, and the Southern Oscillation. *J. Climate*, **3**, 163-170.
- Philander, S.G., 1990: *El Niño, La Niña, and the Southern Oscillation*. American Press, Inc., 293 pp.
- Preisendorfer, R.W., 1988: *Developments in atmospheric science 17: Principal component analysis in meteorology and oceanography*. Elsevier Science Publishers B.V., 425 pp.
- Pittock, A.B., 1975: Climate change and the pattern of variation in Australian rainfall. *Search*, **6**, 498-503.
- Priestley, C.H.B., 1962: Some lag associations in Darwin pressure and rainfall. *Aust. Met. Mag.*, **38**, 32-42.
- Priestley, C.H.B., 1964: Rainfall - sea-surface temperature associations on the New South Wales coast. *Aust. Met. Mag.*, **47**, 15-25.
- Priestley, C.H.B. and A.J. Troup, 1966: Droughts and wet periods and their association with sea-surface temperature. *Aust. J. Sci.*, **29**, 56-57.
- Quayle, E.T., 1929: Long range rainfall forecasting from (Darwin) air pressures. *Proc. R. Soc. Victoria*, **41**, 160-164.
- Quayle, E.T., 1929: Long range rainfall forecasting from (Darwin) air pressures. *Proc. R. Soc. Victoria*, **41**, 160-164.

- Richman, M.B., 1986: Rotation of principal components. *J. Climatol.*, **6**, 293-335.
- Ropelewski, C.F. and M.S. Halpert, 1987: Global and regional scale precipitation patterns associated with the Southern Oscillation/El Niño. *Mon. Wea. Rev.*, **115**, 1606-1626.
- Slutz, R.J., T.J. Lubker, J.D. Hiscox, S.D. Woodruff, R.L. Jenne, D.H. Joseph, P.M. Steurer and J.D. Elms, 1985: COADS Comprehensive Ocean-Atmosphere Data Set Release 1, CIRES University of Colorado, 300 pp.
- Srikanthan, R. and Stewart, B.J., 1991: Analysis of Australian rainfall data with respect to climate variability and change. *Aust. Met. Mag.*, **39**, 11-20.
- Streten, N.A., 1981: Southern Hemisphere sea-surface temperature variability and apparent associations with Australian rainfall. *J. Geophys. Res.*, **86**, 485-497.
- Streten, N.A., 1983: Extreme distributions of Australian annual rainfall in relation to sea-surface temperature. *J. Climatol.*, **3**, 143-153.
- Trenberth, K.E., 1975: A quasi-biennial standing wave in the Southern Hemisphere and interrelations with sea-surface temperature. *Quart. J. Roy. Meteor. Soc.*, **101**, 55-74.
- Troup, A.J., 1965: The Southern Oscillation. *Quart. J. Roy. Meteor. Soc.*, **91**, 490-506.
- Walsh, J.E., M.B. Richman and D.W. Allen, 1982: Spatial coherence of monthly precipitation in the United States., *Mon. Wea. Rev.*, **110**, 272-286.
- Whetton, P.H., 1990: Relationships between monthly anomalies of Australian region sea-surface temperature and Victorian rainfall. *Aust. Met. Mag.*, **38**, 31-41.
- Wright, P.B., 1974a: Seasonal rainfall in Southwestern Australia and the general circulation. *Mon. Wea. Rev.*, **102**, 219-232.
- Wright, P.B., 1974b: Temporal variations in seasonal rainfalls in southwestern Australia. *Mon. Wea. Rev.*, **102**, 233-243.
- Zhang, X.-G. and T.M. Casey, 1992: Long-term variations in the Southern Oscillation and relationships with Australian rainfall. *Aust. Met. Mag.* **40** 211-225
- Zhang, X.-G. and T.M. Casey, 1992: Long-term variations in the Southern Oscillation and relationships with Australian rainfall. *Aust. Met. Mag.*, **40**, 211-225.



## BIOGRAPHICAL SKETCH

Kenneth Ekers was born in Heidelberg, Germany on June 17, 1968. He was the last of three children born to John and Margaret Ekers. Ken graduated from Clover Hill High School in June 1986 and immediately joined the United States Army. He spent three years as a field artillery meteorologist providing upper air support to training artillery units in Europe before continuing his education at Florida State University in June of 1989. Ken remained an active reservist in the 400th MP POW Camp in Tallahassee, Florida until he was re-activated to the US Army for Operation Desert Storm. Ken served the first six months of 1991 in the Persian Gulf as a military police non-commissioned officer where he processed and guarded prisoners of war amongst other police duties. In August of 1991, Ken returned to Florida State University where he completed his Bachelor of Science in meteorology in May 1993. While studying at FSU, Ken met and married his lovely wife, Heather M. Miller. They remained at FSU where Ken completed his Master of Science in meteorology in May of 1995. Upon completion of the M.S., Ken and Heather look forward to work in the civilian sector.

central sections of Australia are the first areas affected by an ENSO event. In fact these correlations suggest negative (positive) rainfall anomalies in central and northeastern Australia lead positive (negative) Pacific SST anomalies by approximately one to two months. The maximum influence of ENSO affects the southeast regions four to five months later and the correlations suggest the northwest encounters this ENSO influence about four months thereafter.

Philander (1990) suggests that most warm episodes begin around the same time of year; typically El Niño begins in the early months of the calendar year. There is an exception for the cool event (El Viejo) as there exists less similarities between different El Viejo episodes. Thus, it is difficult to determine the exact time of year ENSO influences the rainfall in Australia. Ropelewski and Halpert (1987) show the central and northeastern sections of Australia begin to encounter the effects of ENSO in autumn (March) of the ENSO year, but suggest that these effects may begin as early as January or February. If this is indeed the case, then our lagged correlations suggest that the maximum influence of an ENSO event in the southeast occurs around June or July; the time of maximum seasonal rainfall. Our correlations suggest further that the maximum effects of ENSO are encountered in the northwest region (Region1) in late spring to early summer (October) while the influence of ENSO decreases to the southeast. McBride and Nicholls (1983) concluded that northern rainfall is closely related to ENSO in spring and summer but more so in spring. It appears as if the ENSO influence is greatest in the areas of maximum seasonal rainfall during the ENSO year. Ropelewski and Halpert (1987) concluded these phase patterns of ENSO effects weaken considerably over the entire continent by the following March (about 12-13 months after the

effects begin). Nicholls (1992) stated that many Australian droughts and extensive wet periods tend to last about twelve months. Thus, it appears the effects of ENSO on Australia last about one year.

Significant correlations between the second EOF mode of regional Australian rainfall to the JMA index occur around lags of  $\pm 2$  months for most regions of this study (Table 7). Thus, it appears as if the effects of ENSO are evident in this mode of Australian rainfall. It may be that the local synoptic variability due to the circulation patterns, which are evident in the second EOF mode in many of the regions (section 4.1), are influenced by ENSO.

The correlation of the second EOF mode of the southwest region (Region4) to the ENSO index is found to be the largest correlation (-.59) between rainfall and SST anomalies in the eastern Pacific. The second EOF mode of rainfall in this region is found to be associated with summer rainfall along the southern section of southwest Australia; an increase in SST anomalies over the eastern equatorial Pacific Ocean is followed one month later by a decrease in rainfall anomalies. Wright (1974a) found the SOI is well correlated with the anomalous winter rainfall. Thus, ENSO is associated with both summer and winter rainfall in southwest Australia.

Also notable are the weaker correlations associated with the eastern regions as compared to the central regions. Pittock (1975) displayed largest correlations (exceeding 0.5) for the eastern sections of the continent. McBride and Nicholls (1983) concluded that there has been a westward shift in the maximum correlation between Australia district rainfall and Darwin pressure between two 20 year study periods (1933-1953 and 1954-1974). This study confirms that the maximum correlations in the first mode are pressure between two 20 year study periods (1933-1953 and 1954-1974). This study confirms that the maximum correlations in the first mode are located in the central regions of this study (Region6, Region7 and Region8)

Table 7. Same as in Table 6 except for Australian rainfall (PC2). Region 4 rainfall anomalies show the most impressive relationship with the ENSO indicator.

REGION	Maximum Correlation	LEAD/LAG
1	-.26	-12 & +12
2	.24	+12
3	<u>-.33</u>	+1
4	<u>-.59</u>	-1
5	<u>-.36</u>	+1
6	.15	-6
7	<u>-.36</u>	+2
8	-.26	+1
9	<u>-.46</u>	0
10	<u>-.46</u>	-4

while weaker, yet significant, correlations still remain over eastern Australia.



## CHAPTER 5

### SUMMARY AND CONCLUSIONS

Over 3000 rainfall stations over the Australian continent were used to examine a relationship between evaporative latent heat flux in the Southern Indian Ocean and rainfall in Australia. This study separated the stations into ten distinct seasonal rainfall regions and filtered each station's time series with a twelve month running mean to focus on interannual time scales. An empirical orthogonal function analysis followed by a varimax orthogonal rotation was applied to the data to determine the dominant spatial and temporal variability patterns of each region. A similar process was performed for the LHF of a southern region of the Indian Ocean. The temporal patterns of the first two modes of the rotated EOFs for the rainfall regions were correlated with the temporal patterns of the first two rotated modes of the LHF EOFs. An ENSO index was then correlated with the PCs of the LHF region. Correlation coefficients between the ENSO index and the rainfall regions were also calculated to detect the inconsistencies between the effects of warm (cool) ENSO episodes on Australian rainfall.

The main results of this study follow:

- 1) There is a possible relationship between western Australian rainfall and LHF in the central Indian Ocean. The cause of this relationship is unknown but may be due to the circulation anomalies associated with the southeast trades. Another association between the anomalies of LHF off the western coast of Australia and Australian rainfall anomalies in the central and eastern regions was detected. Since this mode of LHF is significantly

correlated with the JMA index (-.51 at zero lag) (i.e. positive SST anomalies in the eastern equatorial Pacific indicate negative anomalies in LHF off the western coast of Australia), we removed the effects of ENSO to determine if this phenomenon is responsible for the rainfall-LHF relationship. The correlations between the rainfall and LHF improved slightly, but did not change the interpretable results. Thus, ENSO is not considered responsible for the LHF-rainfall relationship.

2) The southwest region (Region4) of Australia is found to have a distinct negative trend in summer rainfall since the early 1960s. A negative trend was previously found for winter rainfall in this region for a similar time period (Allan and Haylock, 1993). Both summer and winter rainfall anomalies for Region4 are found to be associated with ENSO.

3) The rainfall anomalies for stations near Lake Eyre in the central regions of this study show a stronger relationship with ENSO anomalies than do the rainfall anomalies in the eastern and southeastern regions. Thus, the influence of ENSO appears to affect a more central section of the continent than the eastern sections as concluded by Pittock (1975). This apparent 'shift' in the effects of ENSO on Australian rainfall is attributable to the time period of this study.

4) There appears to be a seasonal migration of Australian rainfall anomalies associated with ENSO events. The central and northeast regions appear to initially encounter anomalous rainfall patterns during the southern hemisphere seasons of late summer to early autumn in a given ENSO year. Four to five months later (winter to late winter), ENSO influences the rainfall anomalies in the east and southeast regions. The northwest region encounters the effects of ENSO approximately four months after that (late spring).

5) There appear to be several oscillations associated with ENSO which are evident in Australian rainfall records: a) a significant QBO is evident in all ENSO related rainfall PCs, b) a lower frequency of three years is apparent in the central and northeast region rainfall records, c) the southwest PCs contain a three to four year oscillation while the southcentral and southeast PCs are modulated by a three to six year oscillation and d) a seven year oscillation is found to dominate the rainfall variation in the northwest sections of the continent. This frequency is also noted in eastern Australia. Most of the southern regions of this study show a combination of these distinct lower frequencies.

Although only a weak relationship was found between Australian rainfall anomalies and Indian Ocean LHF anomalies, a limited oceanic region was used. Thus, an extension of the LHF domain, to include more southern latitudes, may prove valuable in future studies in determining a more direct effect of LHF on rainfall variability in Australia. Also, the use of LHF data for the entire Indian Ocean basin may provide teleconnection patterns which are useful for forecasting wet and dry periods throughout the continent. Additionally, other sources of LHF products may aid in producing favorable results.

Further connections between ENSO and rainfall fluctuations in Australia are found in this study. Apparent shifts in the relationship between ENSO and Australian rainfall encourages the use of the most recent data available for forecasting significance. A perception of future shifts and the conspicuous 'migration' of the ENSO influence should remain a concern when utilization of this relationship is practiced in forecasting seasonal rainfall for Australia. The migration of the ENSO influence should remain a concern when utilization of this relationship is practiced in forecasting seasonal rainfall for Australia.

## APPENDIX A

### EOF ANALYSIS

This appendix is a discussion on some of the important properties of EOF analysis and presents the mathematics involved. The orientation of the data array for an EOF analysis (e.g. to order the data row-wise or column-wise) offers no advantages for unrotated eigenvectors except for the possible reduction in the dimensions of the dispersion matrix. The EOF analysis method partitions the spatiotemporal data variance into orthogonal spatial fields and associated temporal patterns which are common among both possible modes of analysis (S or T as discussed in Section 3.1.a) with fixed parameters. This study utilizes the S-mode analysis which isolates subgroups of stations which vary similarly. The example below illustrates the technique for a two-dimensional real-valued data array,  $D$ . The EOF analysis partitions the variance of the data,  $D$ , through its dispersion (covariance) matrix,  $C$ . The EOF analysis technique concentrates on the diagonal elements (variance of the data) of  $C$ ; however, the off-diagonal elements (covariance of the data) are well represented in the first few EOF spatial fields (Jolliffe, 1986).

The calculations of the eigenfunctions and eigenvalues have been done with LAPACK (Linear Algebra PACKage) and BLAS (Basic Linear Algebra Subprograms) routines. The study presents a simple symbolic mathematical procedure of the technique. A more thorough discussion is found in Preisendorfer (1988).

The EOF procedure begins with the calculation of the two-dimensional real-valued spatial covariance matrix,  $C$ , found in Preisendorfer (1988).

The EOF procedure begins with the calculation of the two-dimensional real-valued spatial covariance matrix,  $C$ .

$$C = (D \cdot D^T) / (N - 1) \quad (1)$$

where  $N$  represents the number of temporal observations,  $( )^T$  indicates the transpose and  $D$  is the data array with  $M$  rows and  $N$  columns ( $M$  is the number of spatial locations,  $N$  is the number of temporal records). The EOFs are calculated from a solution of the eigensystem equation:

$$CV = \lambda V \quad (2)$$

where  $\lambda$  is the eigenvalue vector and  $V$  is the eigenvector (or EOF) matrix. The eigensystem equation can be written as:

$$(C - \lambda I)V = 0 \quad (3)$$

where  $I$  is the identity matrix. From linear algebra, a nontrivial  $V$  requires:

$$\det[C - \lambda I] = 0 \quad (4)$$

$C - \lambda I$  is a two dimensional square matrix ( $j \times j$ ) whose main diagonal is  $C_{jj} - \lambda$ . Thus, the determinant of  $C - \lambda I$  is a  $j^{\text{th}}$  order polynomial whose roots are the solution to the eigenvalues. Once a  $\lambda$  is known, an associated eigenvector (EOF) is determined. The  $j$  eigenvectors form an orthonormal basis set which can represent the data. Normalized eigenvalues each represent a percent of the variance of the analyzed data set. The largest eigenvalue is considered the most important since it accounts for more



variance and thus its associated EOF is labeled as the first EOF (EOF1). The next largest eigenvalue is labeled the second EOF (EOF2) and so on. The analysis concludes by solving for the time series associated with each eigenvector by projecting the eigenvectors back onto the data:

$$V^T \cdot D = T^T \quad (5)$$

where  $( )^T$  is the transpose of the matrix and  $T$  is the temporal matrix of the EOF analysis. Thus the results is  $M$  eigenvectors (EOFs), each with  $M$  elements representing each of the spatially located stations. Associated with each EOF is an  $N$ -element vector time series which modulates the spatial pattern.

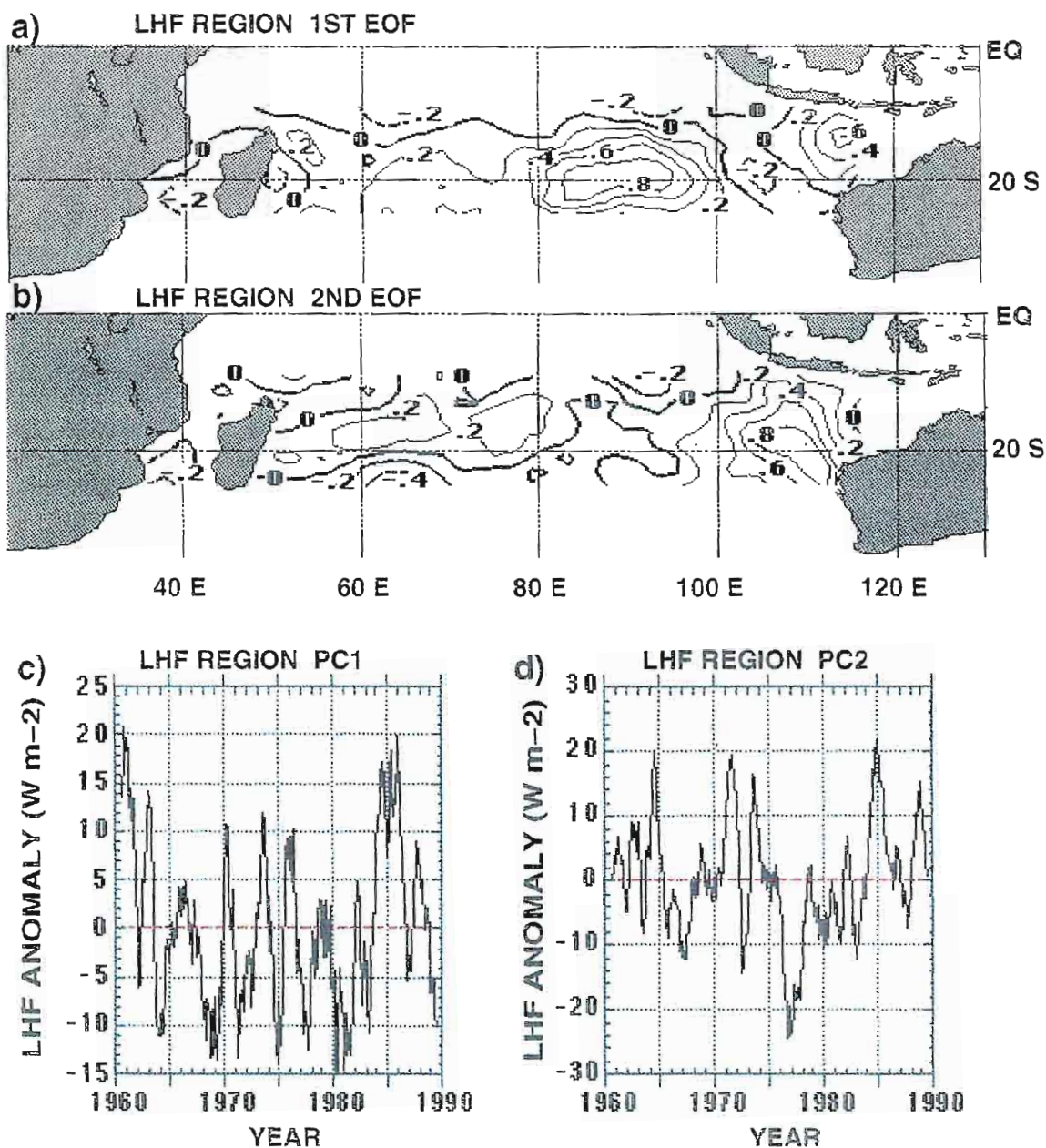


Fig. 16: a) The first rotated spatial field (EOF1) of normalized station loadings for the LHF region. b) Same as in (a) except for EOF2. c) The associated time series of EOF1(PC1) and d) the associated time series of EOF2 (PC2).

Fig. 16: a) The first rotated spatial field (EOF1) of normalized station loadings for the LHF region. b) Same as in (a) except for EOF2. c) The associated time series of EOF1(PC1) and d) the associated time series of EOF2 (PC2). The PCs display LHF anomalies in units of watts per meter squared ( $W m^{-2}$ ).

10°S. During late March to early April, the winds in this area weaken considerably only to regain maximum strength by June. This EOF mode is modulated by a strong QBO interacting with a lower frequency of five years.

### 4.3 Cross Correlations

This study utilizes the cross correlation method to detect and illustrate any relationships between two variables of interest. In particular it determines which variable temporally leads or lags the other variable. Correlation significance is determined through the use of a Monte Carlo procedure (pers. comm. J. Elsner). One thousand surrogates of the first variable PC to be correlated are generated using an Auto Regressive (AR) model. Each surrogate is correlated with the PC of the second variable. A rank of these one thousand correlation coefficients allows for a confidence interval at each lead/lag. Recall each PC consists of 30 years of monthly mean data filtered with a 12 month running mean for a total of 349 points.

#### 4.3.1 Relationship between LHF and JMA

It is of interest to note that Jones et al. (1994) found no significant correlation between Indian Ocean LHF and ENSO. This study correlates LHF in the Southern Indian Ocean and the JMA index to determine if similar results are obtained. The first mode of LHF (EOF1) shows no significant correlation with ENSO (i.e. the JMA index), however, the second mode shows a strong relationship with the ENSO indicator. A correlation coefficient of -.51 was found at a lag of 0 (significant at the 99% level). This indicates that LHF for the mode displayed by EOF2 occurs simultaneously with the warming of SSTs in the eastern equatorial Pacific Ocean. Thus,

when El Niño (El Viejo) associated positive (negative) SST anomalies occur in the equatorial Pacific, negative (positive) anomalies in LHF occur near northwest Australia and in the western Indian Ocean region of interest. This suggests a negative (positive) anomaly of the surface wind over much of the Southern Indian Ocean during an El Niño (El Viejo) event.

#### 4.3.2 *Relationship between Rainfall and LHF*

This study hypothesizes the direct causal effect of Indian Ocean LHF on Australian rainfall. Thus expectations of strong simultaneous correlations exist between these two variables. The correlations of the first two significant PCs for each rainfall region are correlated with the first two significant PCs from the LHF region for a total of 40 correlations. Recall, this study is correlating filtered time series (twelve month running mean applied to data). Thus, expectations of small deviations in the correlation coefficients from one time step to the next exists. A 95% confidence interval (CI) (as discussed in 4.3a) applied to the correlation coefficients immediately indicates that a relationship between LHF and Australian rainfall is not apparent (Tables 2-5).

There are significant correlations (.35 -.43) between Region6 PC2 and LHF PC2 at a lag of four to twelve months indicating that positive LHF anomalies lead rainfall anomalies in this region by four months to a year. It does not seem apparent that LHF is the cause of rainfall variability in this region, but strong correlations which last for nine months (not shown) indicate that there is some connection. A similar result is found for Region9 PC1 and LHF PC2. Anomalous positive LHF off the western coast of Australia precedes positive rainfall anomalies in this region by six to ten months (correlations of .35 -.36). Note, there is once again an extended

Table 2. Maximum correlation coefficient (for lead/lag range of  $\pm 12$  months) between Australian rainfall (PC1) and Indian Ocean LHF (PC1). The lead/lag at which the correlation occurs is also noted. A (-) in the 'LEAD/LAG' column indicates that LHF anomalies lead rainfall anomalies by that many months. An underlined correlation coefficient indicates it is significant at 95% confidence. Note there are no significant correlations in this table.

REGION	Maximum Correlation	LEAD/LAG
1	.24	+7
2	.28	-8
3	.05	+12
4	.18	-9
5	.27	-6
6	.24	-12
7	.16	+2
8	.09	+1
9	.16	+10
10	.12	+1



Table 3. Same as in Table 2 except for Australian rainfall (PC1) and Indian Ocean LHF (PC2).

REGION	Maximum Correlation	LEAD/LAG
1	<u>.35</u>	-10
2	.24	+12
3	.15	-1
4	.24	-5
5	.21	-9
6	.17	+2
7	-.18	-12
8	.23	-1
9	<u>.36</u>	-9
10	.28	-5

Table 4. Same as in Table 2 except for Australian rainfall (PC2) and Indian Ocean LHF (PC1).

REGION	Maximum Correlation	LEAD/LAG
1	<u>.32</u>	-3
2	<u>.33</u>	-12
3	.13	0
4	<u>.36</u>	-12
5	.22	-11
6	.28	+12
7	.23	-7
8	.24	-2
9	.18	+8
10	.30	+8

Table 5. Same as in Table 2 except for Australian rainfall (PC2) and Indian Ocean LHF (PC2).

REGION	Maximum Correlation	LEAD/LAG
1	<u>.34</u>	+12
2	<u>.30</u>	+11
3	.21	-5
4	.23	0
5	.15	+12
6	<u>.43</u>	-10
7	.21	-12
8	.33	0
9	.18	+12
10	.16	-7

period of significant correlations (5 months; not shown). Region1 also shows significant correlations between rainfall PC1 and LHF PC2 (correlation value of .35 at a lag of ten months). Again, LHF does not appear to be the cause of rainfall in these regions, but appears to have some link to the variability patterns.

Since LHF PC2 is correlated with ENSO, it is of interest to calculate the correlation between the time series of rainfall and LHF PC2 without the effects of ENSO. A partial correlation between Region6 PC2 and LHF PC2 (without the ENSO signal) results in a slight improvement in the correlation; the significant correlation coefficients range from .33-.44 with .44 occurring at a lag of ten months. Similar results are obtained for a partial correlation between Region9 PC1 and LHF PC2; significant correlations range from .32-.38 with .38 occurring at a lag of nine to ten months. Notable differences in the correlation between rainfall and LHF PC2 are not incurred when the effects of ENSO are removed, thus the correlations of Australian rainfall and LHF off the northwestern coast of Australia are not due to ENSO, but to other factors.

The significant values of the Region1 PC2-LHF PC1 correlation suggest that an increase in rainfall in this region is preceded by an increase in LHF in the central Indian Ocean by 1-3 months. Although it is not clear why, this is the only (lagged) correlation which suggests a possible direct causal effect of LHF on Australian rainfall. Since the area of LHF EOF1 is representative of the southeast trade winds, it may be that the circulation anomalies associated with these winds and subsequent LHF anomalies are the cause of the relationship indicated. Other significant correlations exist between Region2 PC2-LHF PC1 (correlation of .33 at a lag

of twelve months) and Region4 PC2-LHF PC1 (correlation of .36 at a lag of twelve months).

From the evidence cited above, it is inferred that rainfall in Australia is not directly caused by the evaporative heat flux in the Indian Ocean. The northwest section of the continent (Region1) show lagged correlations around 1-3 months with a maximum correlation occurring at a lag of three months. All other significant rainfall-LHF correlations imply positive LHF anomalies lead positive rainfall anomalies by four to twelve months which is not conducive for a direct effect of evaporative heat flux on rainfall. Several regions of this study do not even show a relationship between rainfall and LHF. This suggests the significant correlations may be a result of circulation anomalies which induce similar patterns to the areas showing significance.

#### 4.3.3 *Relationship between Australian Rainfall and JMA Index*

Cross correlations with a lead-lag of  $\pm 12$  months are also calculated for Australian rainfall and the JMA Index. These correlations should agree with many of the results of other studies which show strong correlation between ENSO and rainfall over the continent (Pittock, 1975; Trenberth, 1975; Angell, 1981; McBride and Nicholls, 1983; Ropelewski and Halpert, 1987 and Nicholls and Kariko, 1992). A 95% CI is applied to the correlations to determine significance.

The significant correlations of the first EOF mode of rainfall for each region of this study with the JMA index indicate a seasonal 'migration' of the effects of ENSO from the northeast and central regions of Australia (Table 6) to the southern regions and then back to the northern regions. The correlations of Region5, Region6 and Region7 indicate that northeast and



Table 6. Maximum correlation coefficient (for lead/lag of  $\pm 12$  months) between Australian rainfall (PC1) and the JMA index. The lead/lag at which the correlation occurs is also noted. A (-) in the 'LEAD/LAG' column indicates negative (positive) SST anomalies in the eastern equatorial Pacific Ocean lead positive (negative) rainfall anomalies by that many months. An underlined correlation coefficient indicates it is significant at 95% confidence.

REGION	Maximum Correlation	LEAD/LAG
1	<u>-.35</u>	-9
2	-.13	+2
3	-.20	0
4	<u>-.34</u>	-3
5	<u>-.38</u>	+2
6	<u>-.41</u>	+1
7	<u>-.41</u>	+1
8	<u>-.45</u>	-4
9	<u>-.36</u>	-5
10	<u>-.40</u>	-4

and then again from February 1975 until March 1976. Allan (1983) noted low level monsoonal circulation is the feature which organized deep convection activity over the continent during 1974; a weaker flow was also noted in 1976. Allan attributes this flow to the variations of the southwest Asian monsoon which is suggested to be associated with with large-scale teleconnection patterns of the (SO). Thus, the rainfall patterns between 1973-1977 were largely influenced by ENSO. Not evident in PC1 is a weaker rainfall event which occurred in 1984 (Allan et al., 1986). The spectrum of Region6 PC1 indicates a significant three year periodicity modulates the spatial field of EOF1. The stations of EOF2 are oriented with positive loadings extending from the northwest to the southcentral sections of this region. Negative loadings are located in the northcentral and extend to the southeast. This indicates a negative relationship between the two areas. All other stations have near zero loadings. This spatial pattern is typical of the influence of synoptic scale systems which cross this region oriented northwest/southeast. Within this signal is a dominant QBO which modulates EOF2.

REGION7 EOF analysis (Figure 12): The mode displayed by EOF1 shows large positive loadings in the north-northeast section of this region. These stations are located directly to the east of the (positive) stations of Region6 EOF1. Since both spatial fields highlight a consistent area of the continent, an immediate indication is that a similar mode is being displayed. This is confirmed in the temporal patterns of PC1. Both PC1s have similar oscillations (i.e. 2 1/2 year periodicity) and both show strong positive anomalies for the 74 and 76 events. Although not as strong in Region6 PC1, Region7 PC1 highlights the 84 event. The north/northwest section of Region7 dominates the mode of EOF2 (i.e. large positive loadings).

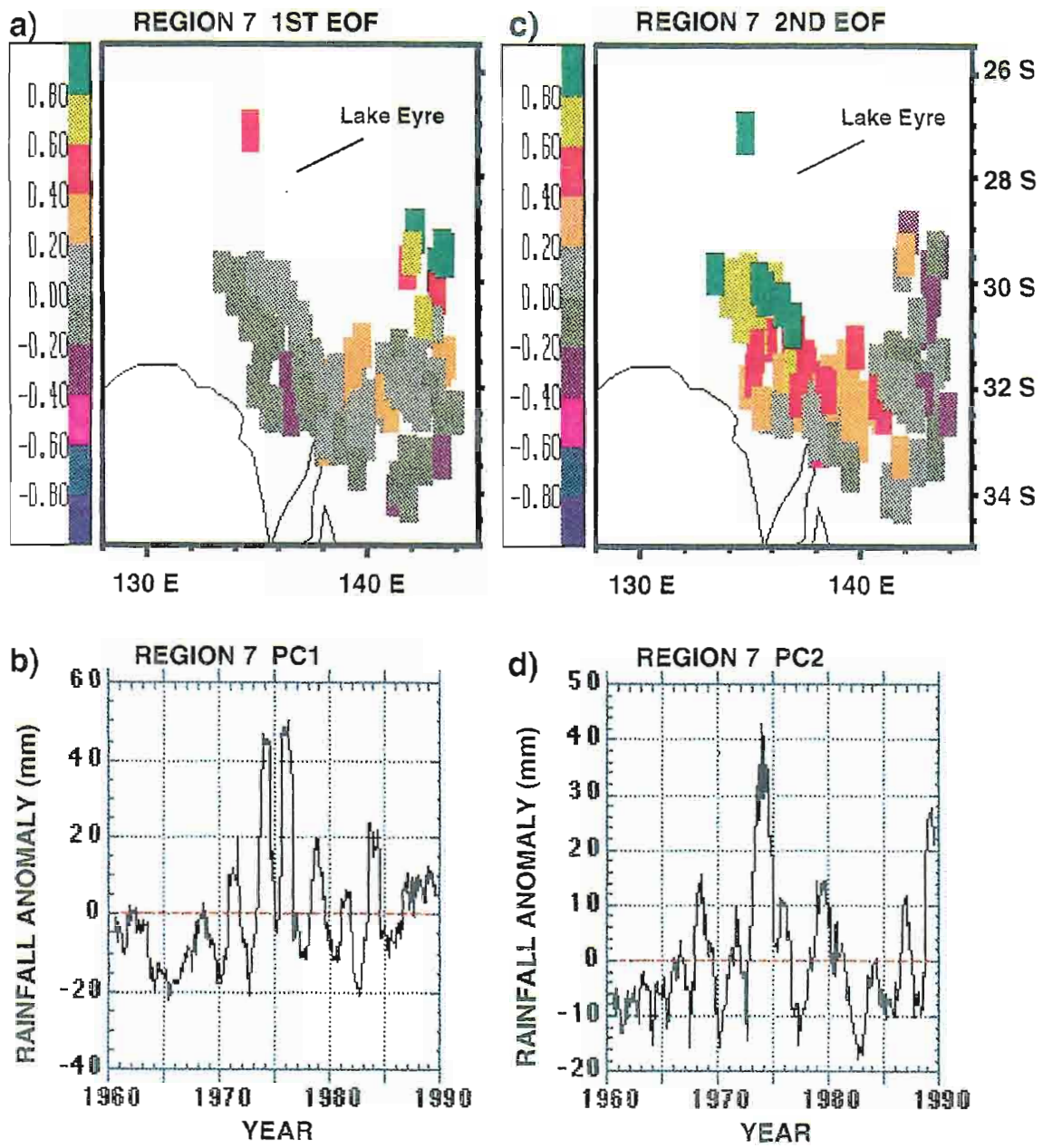


Fig. 12: Same as Figure 6 except for Region 7.

Fig. 12: Same as Figure 6 except for Region 7.

Other smaller loadings indicate the western section as positive and the eastern section as negative. This distribution of EOF values matches well with the patterns in EOF2 of Region6. The time series (PC2s) of each region also possess similar fluctuations (i.e. QBO).

REGION8 EOF analysis (Figure 13): The mode of EOF1 is dominated by the stations southeast of Melbourne. These large positive loadings are influenced by the topography of the region; the Australian Alps which are over 400 m in height are located directly to the north of these stations. Although not extremely high, the topography can help create local weather phenomena (i.e. the southerly buster and the Melbourne eddy) (Baines, 1990). Whetton (1990) suggested that increased rainfall over southeastern Victoria (stations to the southeast of Melbourne) is associated with cold SSTs off the southeastern coast of Australia. This is not what is expected, but is believed to be a response to an atmospheric circulation anomaly. Thus the rainfall pattern of PC1 may be due largely to synoptic conditions. Within the temporal pattern of EOF1 exists several extreme events. The 74 event is an extreme wet episode while 1967 and 1982 show extreme dry anomalies. It is of interest to note that 1967 was an El Viejo year and 1982 was an El Niño year. This indicates that the mode is not related to the ENSO cycle. The power spectrum indicates PC1 has a significant three to five year oscillation which interacts with a QBO. EOF2 isolates the stations with large positive loadings in the extreme western section of this region. These stations are located around Adelaide while most other stations contain values near zero. Drosdowsky (1993c) suggested that summer and autumn SST anomalies off the western coast of Australia can be used to forecast early winter rainfall over parts of eastern and southern Australia. Drosdowsky does not believe the SST anomalies drive the rainfall



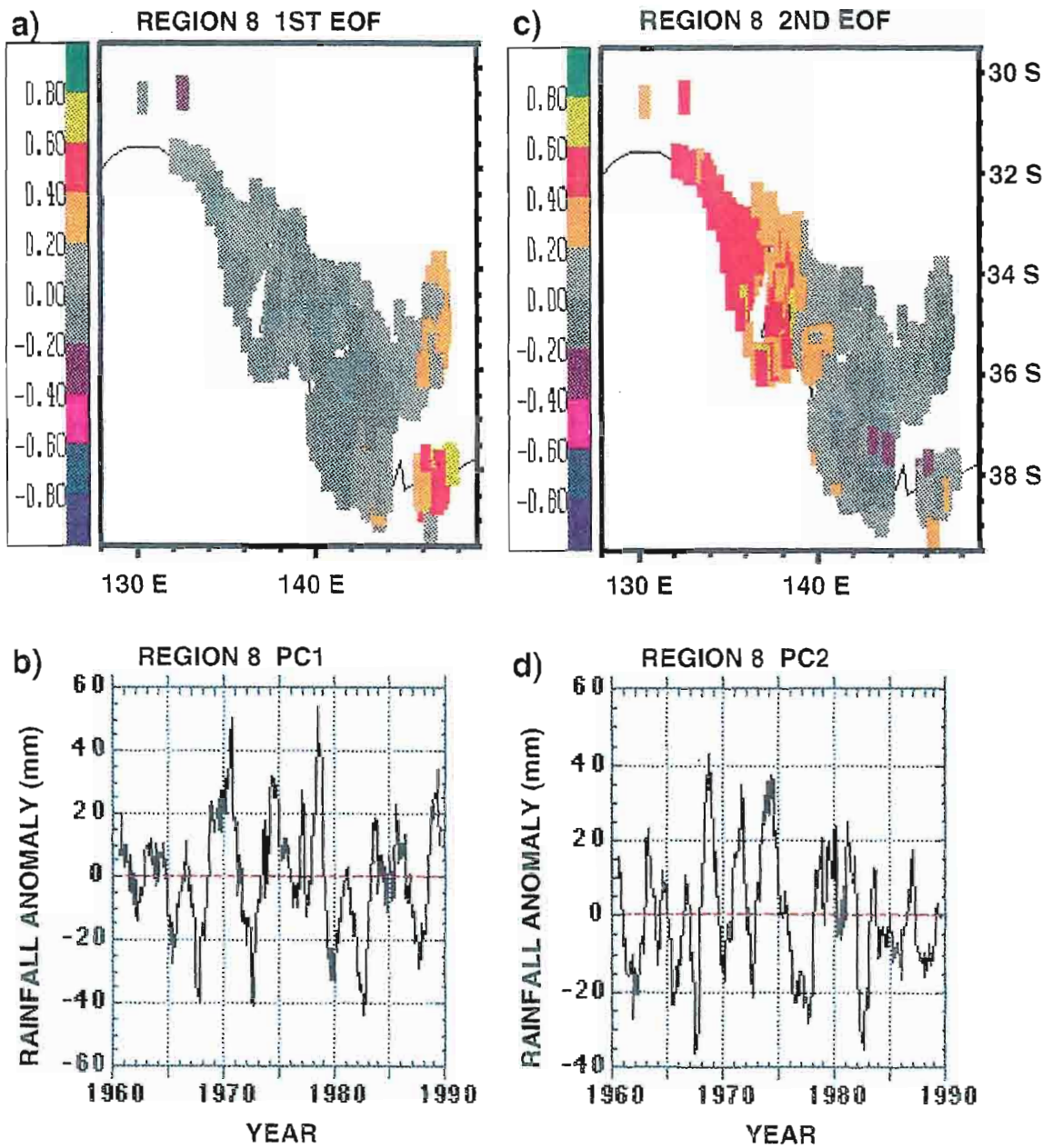


Fig. 13: Same as Figure 6 except for Region 8.

Fig. 13: Same as Figure 6 except for Region 8.



anomalies, but rather both are forced by atmospheric circulation anomalies. This argument agrees with the findings of Nicholls (1989). Nicholls found that rainfall in the south/southeast section of the continent has a large correlation ( $>0.6$ ) with an SST gradient between the central Indian Ocean and Indonesia. He suggested that this gradient which is associated with rainfall from northwest to southeast Australia may be a result of atmospheric circulation changes. Thus the mode of EOF2 may be one of circulation anomalies over the area.

REGION9 EOF analysis (Figure 14); EOF1 displays stations with large positive loadings centered near  $150^{\circ}\text{E}$ - $152^{\circ}\text{E}$  and  $30^{\circ}\text{S}$ - $33^{\circ}\text{S}$ . This is contrasted by an area of large negative loadings centered around  $153^{\circ}\text{E}$  and  $29^{\circ}\text{S}$ . Thus, these two areas have nearly opposite anomaly patterns. The time series of this mode indicates for the stations with positive (negative) loadings a typical dry (wet) season for warm (cold) ENSO events (i.e. 1965 {El Niño}, 1971 {El Viejo}, 1973 {El Viejo} and 1981 {El Niño}). Thus it seems that the signal of EOF1 is related to ENSO. Inspection of the power spectrum of PC1 indicates the dominant frequency is about seven years which interacts with a QBO. The PCs of this study which contain a seven year oscillation appear to be related to ENSO. As discussed earlier in this section for Region1, a seven year oscillation is presumed to be a low frequency indicator of ENSO. EOF2 displays the positive loadings to the extreme north of the region with small values (near zero) to the south. This orientation of stations matches patterns in EOF1 of Region6. After comparing the time series of Region9 PC2 to that of Region6 PC1, it becomes obvious they are very similar.

REGION10 EOF analysis (Figure 15): The mode displayed by EOF1 isolates the stations with large positive loadings around  $149^{\circ}\text{E}$ ,  $32^{\circ}\text{S}$ . Most

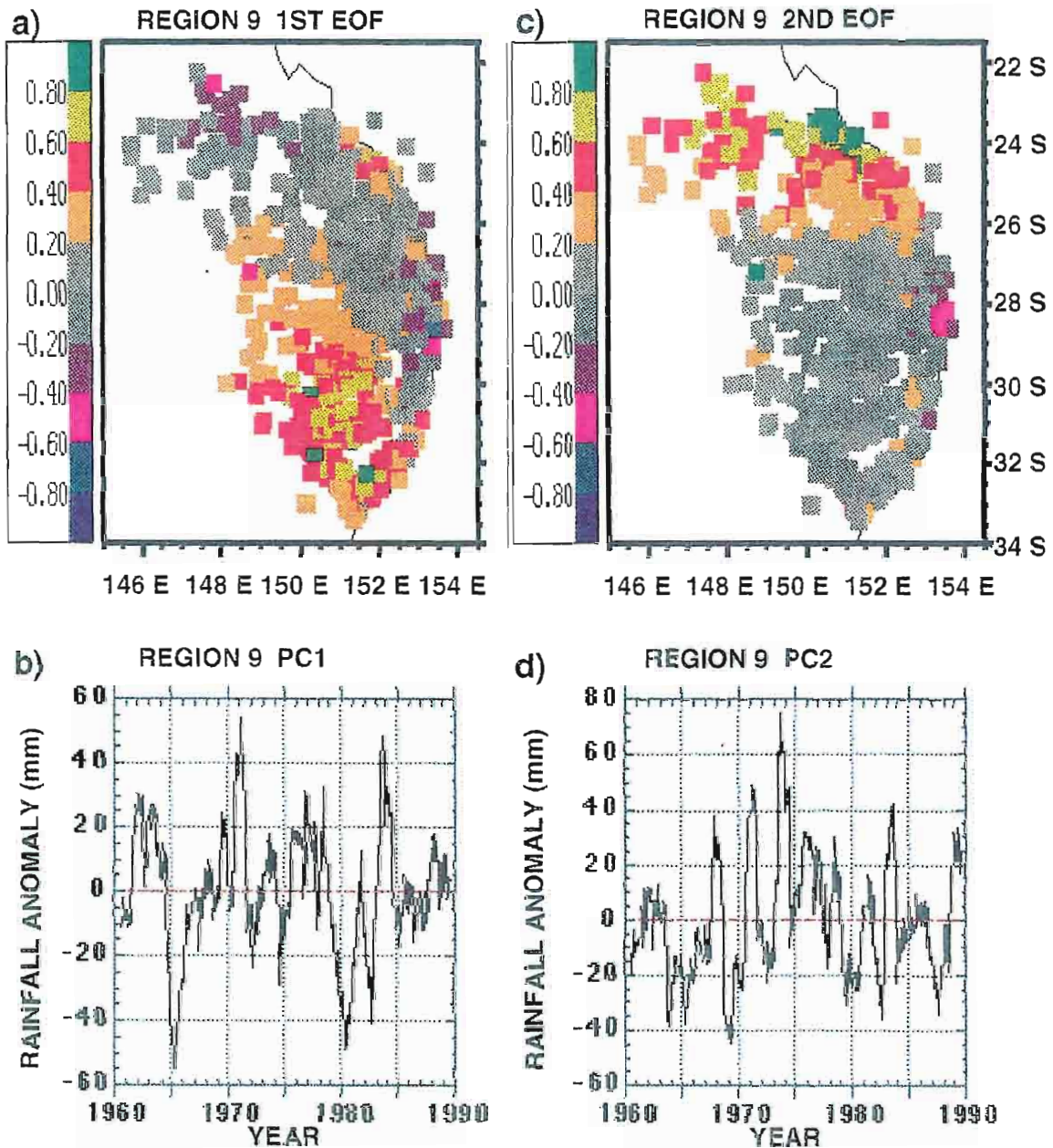


Fig. 14: Same as Figure 6 except for Region 9.

Fig. 14: Same as Figure 6 except for Region 9.

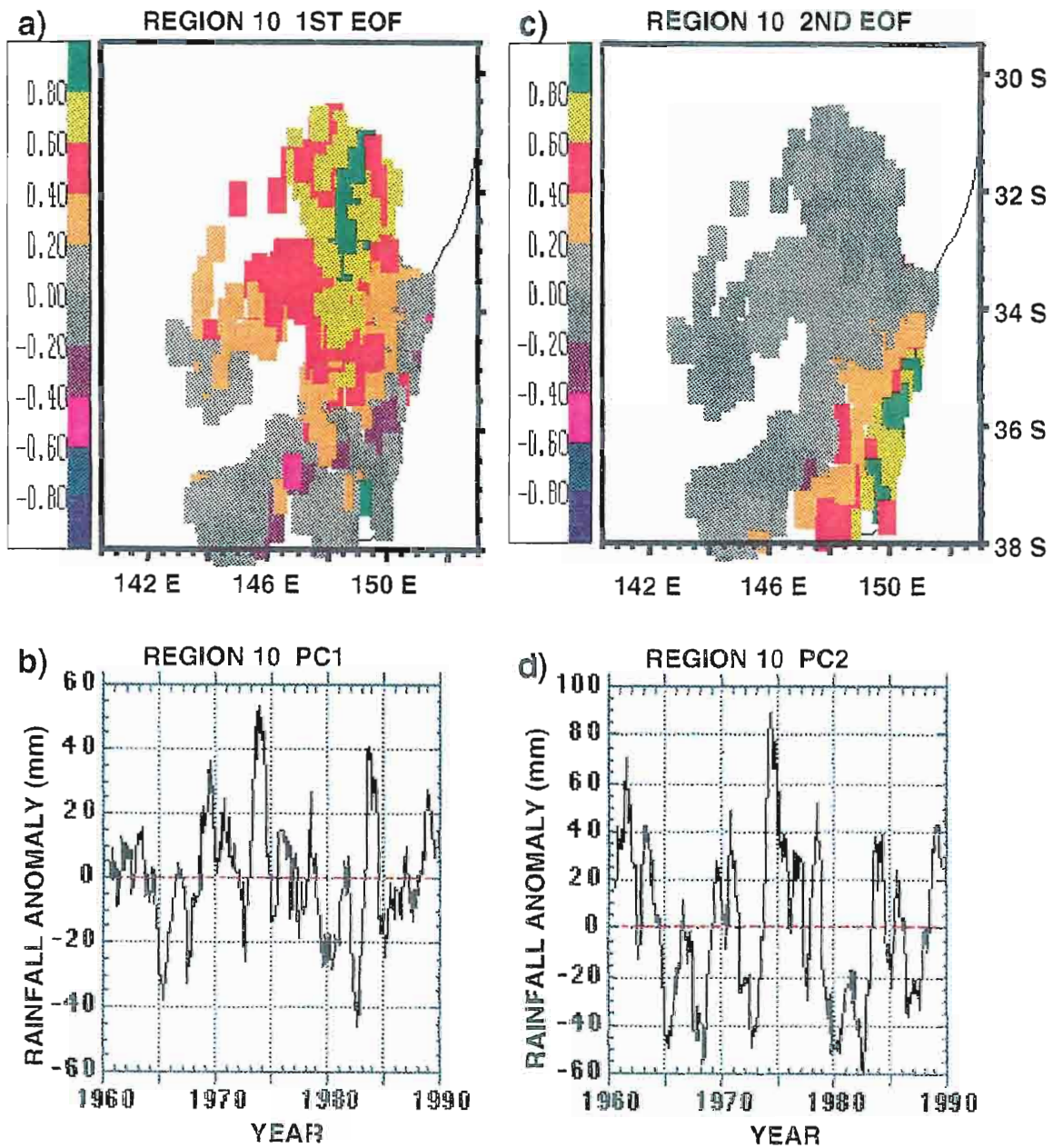


Fig. 15: Same as Figure 6 except for Region 10.

Fig. 15: Same as Figure 6 except for Region 10.



all other stations have small magnitudes. This spatial field matches well with that of Region9 EOF1 (i.e. all large loadings are centered around 146°E-150°E and 30°S-34°S). The time series associated with this spatial field (Region10 PC1) contains a significant QBO and highlights the 74 event. A lower frequency of 3 1/2 years is also found to be significant in PC1. EOF2 concentrates on the stations along the southeast coast of this region. Once again this study shows a relationship between two regions. Region8 EOF1 also has large loadings along the southeast coast in an area which match well with the large loading stations of Region10 EOF2. Recall the Great Dividing Range to the northwest of these stations is a topography feature which causes localized weather phenomena (i.e. the southerly buster) (Baines, 1990). Region10 PC2 indicates a strong QBO and highlights the 74 event; the 76 and 84 event are also evident in the time series. A significant three to five year periodicity is also found in the power spectrum of PC2.

In summary: the EOFs of one region appear to match well with neighboring EOFs (i.e. Region9 EOF2 with Region6 EOF1 with Region7 EOF1) indicating coherent modes of variation. Thus, the domain dependence of unrotated solutions of EOFs as discussed by Richman (1986) has apparently been corrected through the use of the orthogonal varimax rotation. This clearly confirms the positive impact of EOF rotation. Should a delineation of the continent into climatic regions prior to the EOF analysis of rainfall not have been used, the rotated EOF analysis may tend to partition the continent into regional EOF fields based on variation of rainfall as shown by Drosdowsky (1993a).

A QBO (20-30 months) is significant in at least one of the two most significant modes for each region of this study. It appears that this

A QBO (20-30 months) is significant in at least one of the two most significant modes for each region of this study. It appears that this

periodicity is associated with the process of extreme events of ENSO (i.e. El Niño and El Viejo) (Barnett, 1991). A lower frequency of three to seven years interacts with the QBO to affect the regions with oscillating wet and dry periods. The seven year oscillation is dominant in the PCs of the northwest regions (i.e. Region1 and Region2) and also in Region9. Regions which show significant variance due to the three to six year oscillation include those in southern Australia (e.g. Region3, Region4, Region7, Region8 and Region10).

The extreme rainfall events (1974, 1976 and 1984) are not evident in all regions of the continent Allan (1985). Although each PC1 for all regions show the 74 event as a positive (wet) anomaly, a 76 event affected only about 50% of the continent. Typically the north and eastern sections of Australia received above average rainfall for this event. As seen in the time series, the western and southern most regions (Region2, Region3, Region4



regions are located in southern and southwestern sections of the continent. The EOF1 field displayed for these regions differ from each other. Region8 EOF1 is largely indicative of synoptic variability while Region4 EOF1 displays the rainfall pattern of variation due to topography.

Drowsdowsky (1993b) concluded that variation in Australian rainfall patterns is not only influenced by ENSO, but by anomalies in the Southern Hemisphere mid-latitude circulation. The second EOF mode of most regions in this study are rainfall patterns generally resulting from these atmospheric circulation changes and associated changes due to local effects.

#### *4.2 Latent Heat Flux EOFs*

Indian Ocean LHF EOF analysis (Figure 16): EOF1 is dominated by strong positive loadings in the central Indian Ocean region of this study. This mode is indicative of the influence of the strong southeast trade winds. During the Southern Hemisphere winter months, there exist strong east southeasterly winds over the southcentral Indian Ocean while during the summer months the winds weaken and shift to a more northerly component (Miles et al., 1993). EOF1 is modulated by a strong two to three year oscillation.

The second EOF pattern also reflects the influence of winds. The northwest/southeast oriented section of positive anomalies just off the northwest coast of Australia centered on 20°S is reflective of the winds along the western continental coast. During the southern winter the surface winds are strong in magnitude and southeasterly in direction. The winds remain strong and become southerly along the western coast in October. By mid November the winds are southeasterly in direction. The winds remain strong and become southerly along the western coast in October. By mid November (early summer), the strength of the winds off the western coast of Australia weaken slightly and have a westerly direction around

1) The winter rainfall regions of southwestern Australia (WH, WM) are combined to form one region (Region 4).

2) The winter rainfall region in the southeast (WM) remains a separate region (Region 8).

3) The summer tropical (ST), summer arid (AS) and non-seasonal/winter arid (AN) rainfall regions are all subjectively divided into eastern and western rainfall regions (Region 1 and Region 5, Region 2 and Region 6, Region 3 and Region 7, respectively).

4) Tasmania is not included in this study.

5) The two remaining seasonal rainfall regions (SST, U) are unchanged (Region 9, Region 10, respectively).

Thus, the current study encompasses ten Australian seasonal rainfall regions (newly formed regional borders use the closest rainfall district boundaries).

## *2.2 Latent Heat Flux Data Set*

This study uses the Indian Ocean LHF data from Jones et al. (1994). They objectively determined fields of LHF for the Indian Ocean for 1960-1989 utilizing the Comprehensive Ocean-Atmosphere Data Set (COADS) (Slutz et al. 1985). The study region encompasses the area from 30°E-120°E and 29°S-23°N, and data are on a 2° x 2° grid. LHF is not an observed variable; it is based on a bulk aerodynamic formula which relies on monthly mean air temperature, specific humidity and scalar wind speed. The current study focuses on the region 30°E-120°E and 29°S-8°S (Figure 4) and utilizes the 340 grid boxes centered over the ocean in this region for all 360 months of the dataset.

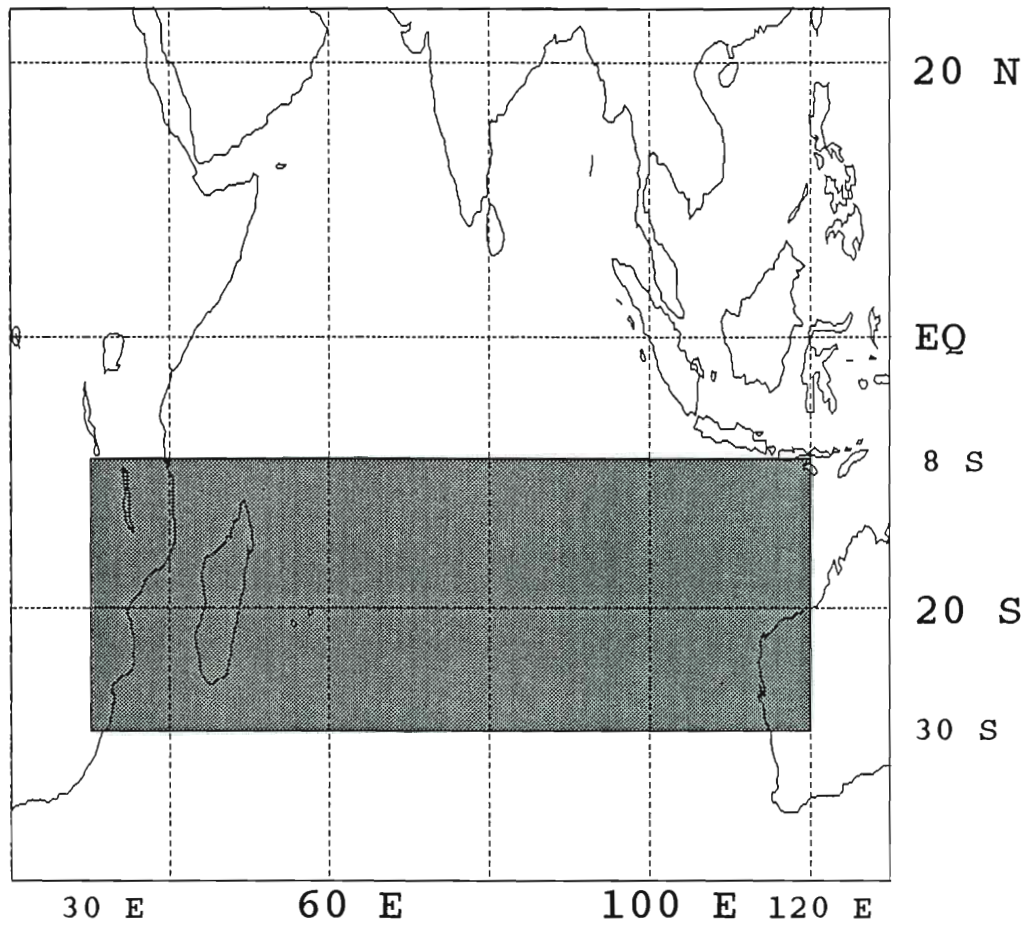


Fig. 4: Geographical region in the Indian Ocean from which latent heat flux (LHF) is used. Data are calculated in Jones et al. (1994).

### *2.3 Japan Meteorological Agency (JMA) Index*

An index based on the SST anomalies in the eastern tropical Pacific Ocean defines the magnitude and timing of the extremes of ENSO (i.e. El Niño, El Viejo). The JMA index is a five month running average of averaged SST anomalies in  $2^{\circ} \times 2^{\circ}$  grid boxes for the region  $4^{\circ}\text{N}$  to  $4^{\circ}\text{S}$  and  $150^{\circ}\text{W}$  to  $90^{\circ}\text{W}$ . A period of SST anomalies of  $+0.5^{\circ}\text{C}$  or more for at least six consecutive months indicates an El Niño period. A counter definition is used to indicate El Viejo periods. The current study applies an additional twelve month running mean to the SST anomalies for the 360-month period 1960 - 1989 (Figure 5) in order to be consistent with processing of other data in this study.

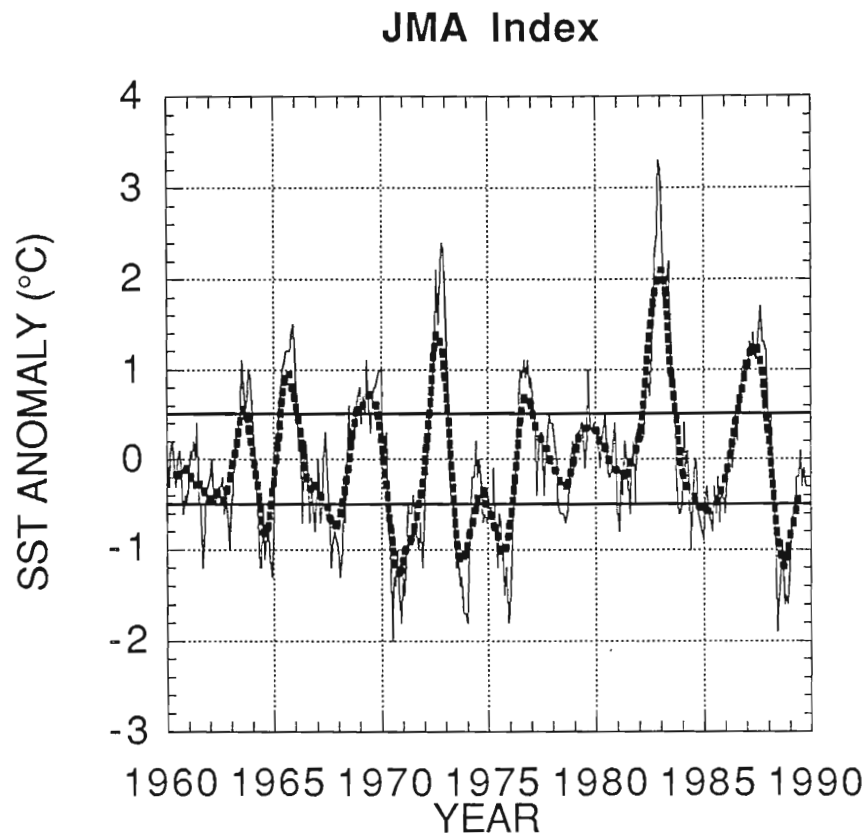


Fig. 5: JMA index (thin solid line) and its 12 month running mean (dashed line). Thick solid lines at  $\pm 0.5^{\circ}\text{C}$  indicate extreme ENSO thresholds (i.e. El Niño  $\{+0.5^{\circ}\text{C}\}$  and El Viejo  $\{-0.5^{\circ}\text{C}\}$ ). Note indications of strongest El Niños in 1972, 1982 and 1986/87.



## CHAPTER 3

### METHOD

The data preparation for the rainfall and LHF data sets are discussed in this section. The first step of preparation includes the removal of all variability with periods shorter than twelve months from each data set; this study's interest is in interannual variability. We also utilize a statistical method to obtain a representative time series for each of the ten Australian rainfall regions and for the Indian Ocean LHF region. An empirical orthogonal function (EOF) or PC analysis for each rainfall and LHF data set is necessary to extract the variability of the data into a set of orthogonal basis functions (i.e. spatial fields and temporal patterns). Finally, all eigenvectors of the EOF analysis that are significant according to a Monte Carlo statistical test (discussed in section 3.3) are 'rotated' to maximize the individual modes of variation.

#### 3.1 *Data Preparation*

##### 3.1.1 *Rainfall*

Eliminating the seasonal frequency fluctuations is accomplished by removing the monthly climatological mean from each station's record. Removing this mean effectively preserves low frequency fluctuations; missing data are then replaced with zeros (i.e. the seasonal mean centered on that month). A twelve month running mean is then applied to each station's record to eliminate intra-annual variability.

An EOF analysis is applied to the data within each region. This requires a matrix to be constructed of the rainfall data where the variables (rows) refer to the stations, the observations (columns) are time series and the parameter (rainfall) is fixed. This specification warrants an S-mode analysis of the data as discussed by Richman (1986). (A T-mode analysis utilizes the transpose of the S-mode analysis data matrix). Each of the ten Australian seasonal rainfall regions are now represented by a two dimensional data array,  $D_i$ ,  $i = 1,10$ .

### 3.1.2 *Latent Heat Flux*

As with the rainfall data, removing the seasonal mean of LHF from each variable for the 30 year period eliminates the annual cycle that is dominant in the Indian Ocean region. There are no missing data values in this data set. Again, a twelve month running mean applied to the LHF data set eliminates higher frequency variability. Preparation of the two-dimensional data array,  $F$ , for the Indian Ocean region of interest for use in the EOF analysis is similar to the rainfall data above. The rows refer to the stations (variables) and the associated time series (observations) are the columns.

## 3.2 *Empirical Orthogonal Function (EOF) Analysis for Rainfall and LHF*

This study performs an EOF analysis on data from each of the ten climatic rainfall regions and from the Indian Ocean LHF region. This analysis produces orthogonal spatial patterns (EOFs) from the eigenvectors of each region's covariance matrix and calculates the associated time series analysis produces orthogonal spatial patterns (EOFs) from the eigenvectors of each region's covariance matrix and calculates the associated time series (PCs) of each EOF. Since there exist a number of solutions which satisfy the eigenmodel equations (Appendix A), mixed modes of variation may result in

the EOF fields; these mixed modes are typically undesirable. Thus for each EOF analysis statistically significant eigenvectors are 'rotated' to find coherent modes of variation. The rules which determine selection of significant EOFs are discussed in section 4. A complete discussion on the properties and mathematics for the EOF analysis is found in Appendix A.

### 3.3 *Rotation of Eigenvectors*

Richman (1986) discussed that unrotated spatial eigenvectors may lead to erroneous interpretations. He mentioned that patterns of unrotated spatial EOFs are predictable. Also mentioned was the possibility of an underlying structure in the data which identifies coherent modes. This structure is known as simple structure; e.g. if values for a station are large for one mode, they should ideally be small for all others. Richman (1986) recommended rotation of significant EOFs as a technique to uncover this hidden pattern in order to obtain the simple structure. Thus this study considers the use of rotation. The percent of variance accounted for by each 'unrotated' EOF is calculated to determine which EOFs are statistically significant. This study utilizes Rule N as discussed by Preisendorfer (1988) which is a Monte Carlo simulation method. Only the statistically significant EOFs are rotated. Each of the rainfall regions and LHF region of this study contain four or more significant eigenvectors with a cumulative variance of more than 70% (Table 1).

There are several types of rotation available as discussed by Richman (1986). He suggested using the varimax orthogonal rotation or the promax k=2 oblique rotation methods for their type (orthogonal, oblique). An EOF analysis was performed on the data set of Region 4 of this study. The

Table 1: Rainfall and LHF regions EOF results. Each of the ten rainfall regions plus the LHF region is utilized in an EOF analysis. The resulting eigenvectors (EOFs) are tested for significance using a Monte Carlo test (see text for full explanation). The significant EOFs account for a cumulative percent of the variant structure of the data for the given region.

REGION	NUMBER OF STATIONS	NUMBER OF SIGNIFICANT EOFs	CUMULATIVE PERCENT OF VARIANCE
1	39	10	89
2	36	9	91
3	107	5	82
4	349	4	79
5	256	4	80
6	184	5	83
7	114	4	88
8	655	4	78
9	828	5	82
10	551	4	81
LHF	340	6	74

unrotated analysis confirmed the spatial fields are predictable as demonstrated by Buell (1975). A varimax orthogonal rotation and a promax  $k=2$  oblique rotation was then applied. A comparative study of the rotated spatial fields demonstrated the two different types of rotation produced similar results. The analytic programs that calculate the rotations are not flawless and thus it is necessary to examine the rotated solutions as suggested by Richman (1986). An examination of the loadings (eigenvector values assigned to the stations) of the significant rotated eigenvectors for each type of rotation is used to determine the quality of simple structure and ultimately decide which of the rotated solutions are usable for this study. The unrotated case results are also examined. The unrotated solution demonstrates virtually no simple structure while the rotated plots reveal a better-defined simple structure. The varimax and promax  $k=2$  rotations produce similar structure and thus this study utilizes the varimax rotation to retain the orthogonality of the eigenvectors. A more in-depth discussion on the rotation of eigenvectors is found in Appendix B.

A visual inspection of the time series for each rotated EOF indicates a large positive trend of LHF variability beginning in the mid to late 1970s. Some of this trend is due to a positive trend in the scalar wind speed which is maximum in the region of the Southern Trades and Arabian Sea (Jones et al., 1994). The increase of wind speeds may not be necessarily due to changes in wind reporting techniques (Cardone et al., 1990) since the trend is largest for high wind speeds; however, it may be due to a change in anemometer heights (pers. comm. D. Legler ). For this study the trend in LHF is considered artificial and is removed. A line was fit to each PC using anemometer heights (pers. comm. D. Legler ). For this study the trend in LHF is considered artificial and is removed. A line was fit to each PC using a least-squares method and then removed from the data.



## CHAPTER 4

### RESULTS AND DISCUSSION

#### 4.1 *Rainfall EOFs*

The rotated eigenvectors of the rainfall regions produce spatial fields which isolate a cluster of stations that vary similarly. The first two EOF spatial fields (EOF1 and EOF2) for each region consist of the majority of the explained variance in the data (typically 60%-70%). Stations are significant in those spatial fields should the magnitude of their loadings exceed 0.40. The associated time series of each spatial field (PC1 and PC2) indicate the modulation of the variant rainfall. Significant oscillation periodicities of these time series are determined from the power spectra. All frequencies which peak above the 95% Markov 'red noise' null hypothesis significance level (Burroughs, 1992) are considered 'significant'. In many cases more than one frequency in a given spectrum is found to peak above the 95% significance level. This suggests more than one oscillation is accountable for generating the time series. Henceforth the term 'interacting' implies this generation occasioned by two or more periodicities. A brief analysis of the EOF pairs (i.e. spatial fields and time series for each region) follows.

REGION1 EOF analysis (Figure 6): The spatial structure of EOF1 isolates a few stations with loadings of amplitude greater than 0.6, i.e. the area between 127°E and 130°E south of Joseph Bonarte Gulf appears to contain the maximum positive amplitude while the two stations centered near 122°E, 11°S around Cape Don display a steep amplitude gradient. PC1 contains interesting periodicities based on the output from its power

of the southwestern region of Australia is an area under particularly strong ENSO influence. Correlations between the anomalies of Australian rainfall and Indian Ocean LHF illustrate the presence of a relationship between rainfall in central Australia and LHF off the western coast of Australia. The LHF-rainfall association is essentially independent of ENSO. This may signify the importance of offshore LHF as a distinct factor besides ENSO influencing the variant structure of Australian rainfall, although the nature of this study does not allow a determination if LHF is a forcing factor.

## CHAPTER 1

### INTRODUCTION

Annual rainfall over Australia is highly variable, but certain patterns of deviation from the average anomaly patterns tend to recur (Pittock, 1975). Thus, a productive search for empirical evidence between Australian rainfall and known physical phenomena might lead to forecast improvements for seasonal precipitation over the continent.

The pioneering studies of Priestley (1964) and Priestley and Troup (1966) linked sea-surface temperature (SST) anomalies to rainfall in Australia. Streten (1981) confirmed these studies by documenting a relationship between above normal SSTs surrounding continental Australia and extreme rainfall events in Australia. A later study by Nicholls (1989) found a significant correlation between the first principal component of winter Australian rainfall and an SST gradient between the central Indian Ocean and Indonesia. Nicholls associated this large correlation to the location of the east coast subtropical ridge, with large scale cloud bands extending northwest-southeast across the continent (i.e. precipitation in the areas under these clouds were most correlated to the SST anomaly gradient). Drosowsky (1993c) examined whether Nicholls' results indicated the rainfall anomalies were an immediate cause of the SST gradient or whether both were a cause of some unknown forcing. He discovered the SST winter dipole pattern in the Indian ocean develops as a result of the atmospheric circulation anomalies. The inability of these studies to find a concrete causal relationship between SSTs in the Indian Ocean and rainfall

fluctuations in Australia necessitates research to study meteorological variables of the Indian Ocean influenced by factors other than SSTs and their relation to Australian rainfall variability, one of the goals of this research. Since SST patterns do show some correlation with rainfall, it is possible that a variable associated with SST but driven by other constituents may be more directly related to the cause of rainfall fluctuations over the continent.

The research in this study utilizes calculated latent heat flux (LHF) monthly mean values from January 1960 through December 1989 in the Indian Ocean obtained from Jones et al. (1994). LHF is correlated with winds over the Indian Ocean. The trade wind region east of Madagascar indicates lower SSTs when the winds are stronger than normal. This subsequently produces higher LHF in the area. Additionally, wind speed and not the SSTs are more influential in the variability of LHF. Thus, LHF is related to wind speeds with some association to SSTs.

The focus of this study is to evaluate the variability of multiple individual rainfall stations in each of ten climatological Australian rainfall regions and to determine their relationship with the variation of LHF in the southern Indian Ocean. An empirical orthogonal function (EOF) analysis and an orthogonal rotation to the varimax criterion is implemented to highlight these relationships. No other study has attempted to correlate LHF in any oceanic region with Australian rainfall.

Jones et al. (1994) concluded there is not a strong correlation between LHF in the Indian Ocean and El Niño. There is, however, evidence of a relationship between Australian rainfall variability and the El Niño/Southern Oscillation (ENSO). The relationship observed between Australian rainfall and ENSO was identified by Quayle (1929). Quayle

indicated an increase in Darwin pressure anomalies were followed by a decrease in the rainfall anomalies for northern and eastern Australia. Others (e.g. Priestly 1962; Troup 1965; Pittock 1975; Nicholls and Woodcock 1981; McBride and Nicholls 1983; Ropelewski and Halpert 1987) have explored further a relationship between rainfall in Australia and the Southern Oscillation (SO) index, an index of pressure anomalies between Tahiti and Darwin. Ropelewski and Halpert (1987) confirmed most previous studies by documenting that El Niño years (large negative SO index values) are associated with dry years in Australia. Nicholls (1989) found that rainfall stations affected by ENSO had higher relative variability than those stations not affected by ENSO. All of these studies determined the effect of ENSO on Australian rainfall variability based on the pressure anomaly difference between Tahiti and Darwin. The current study utilizes the Japanese Meteorological Agency (JMA) SST index to determine the relationship between ENSO events and fluctuations of Australian rainfall. The JMA is an eastern equatorial Pacific Ocean SST anomaly-based index which highlights ENSO events. This SST based index indicates the occurrence of every El Niño and El Viejo event.

Our principle interest lies in the (unknown) Indian Ocean LHF-Australian rainfall relationship. As Nicholls (1989) discussed, not every extreme ENSO event produced similar rainfall patterns over Australia; some events (e.g. 1970-1971 El Viejo) produced weak rainfall anomalies while others (e.g. 1973-1974 El Viejo) produced strong variation in the rainfall over the continent. Perhaps LHF is an influential parameter of Australian rainfall not associated with ENSO which can help explain the rainfall over the continent. Perhaps LHF is an influential parameter of Australian rainfall not associated with ENSO which can help explain the inconsistent rainfall anomaly patterns associated with ENSO. This is one of the possibilities to be examined in this study.



Section 2 of this study describes the Australian rainfall, Indian Ocean LHF and JMA index data sets and delineates the ten climatological Australian rainfall regions. Preparation of the data includes sub-sections on discussions of the EOF analysis and the rotation of eigenvectors as discussed in Section 3. The results and discussion of this study are presented in Section 4 with a summary and closing remarks in Section 5.

## CHAPTER 2

### DATA

#### *2.1 Australian Rainfall Data Set*

This study utilizes Australian rainfall data obtained from the Australian Bureau of Meteorology (BOM). The data are monthly totals of rainfall in millimeters for over 20,000 stations with some individual station records dating back to the late 1800s. Only stations with records covering the thirty year period (1960 - 1989) are included in this study; however, stations not considered part of mainland Australia (such as Tasmania) are eliminated.

Deceptive results may be incurred with studies utilizing records of rainfall stations with known inhomogenities. An analysis (discussed below) to determine the quality of the data set for this study employs a reliable data set, data without spurious trends or inhomogeneities, identified by Lavery et al. (1992). They compiled a list of 191 Australian rainfall stations with continuous records which begin in 1910. The higher quality, long-term stations compiled by Lavery exhibit a limited spatial coverage of Australia not conducive for the current study. Documentation necessary to establish the selected data for this research as consistent and homogeneous were not available. (The terms consistent and homogeneous, as discussed by Srikanthan and Stewart (1991) and Lavery, refer to the instrument types and exposure as well as observational practices and site location for each station over the course of the study period). Therefore, the need to justify the expanded data set in this study is necessary.

A principal component (PC) analysis of the higher quality station records identified by Lavery and the station records for the period 1960 - 1989 justifies the use of the expanded data set in this study. The patterns and magnitudes of the first four PC's of 349 stations in southwestern Australia selected for this study were compared against the same PC's of the 34 stations identified by Lavery in the same region. A visual inspection of each PC1 (first principal component) which accounts for more than half of the variance in the data for each data set indicates nearly indistinguishable differences (Figure 1). The magnitude of the various peaks in the PC patterns are nearly identical; the differences may be due to variability inherent in the additional stations selected for this study. Thus, the PCs of the rainfall stations which meet our 30-year criteria can be analyzed with some confidence.

The station rainfall records chosen for this study consist of data values ranging from less than one millimeter per month to more than 700 millimeters per month. The variability of rainfall over the continent compels a partitioning of the continent into climatic rainfall sectors to allow for analysis without the bias of extreme climates. Srikanthan and Stewart (1991) divided Australia into eight seasonal rainfall regions based on the Bureau of Meteorology (1975) seasonal rainfall zones (Figure 2). A test (not shown) establishing a clear correlation between Indian Ocean LHF and eastern/western Australia rainfall indicates distinct differences between the rainfall regimes in the eastern and western regions of Australia rainfall. Thus, this study redraws the boundaries set by Srikanthan and Stewart to allow for distinct eastern and western regions (i.e. Figure 3). The ~~redistricting~~, this study redraws the boundaries set by Srikanthan and Stewart to allow for distinct eastern and western regions (i.e. Figure 3). The redistricting of the seasonal rainfall regions are as follows:

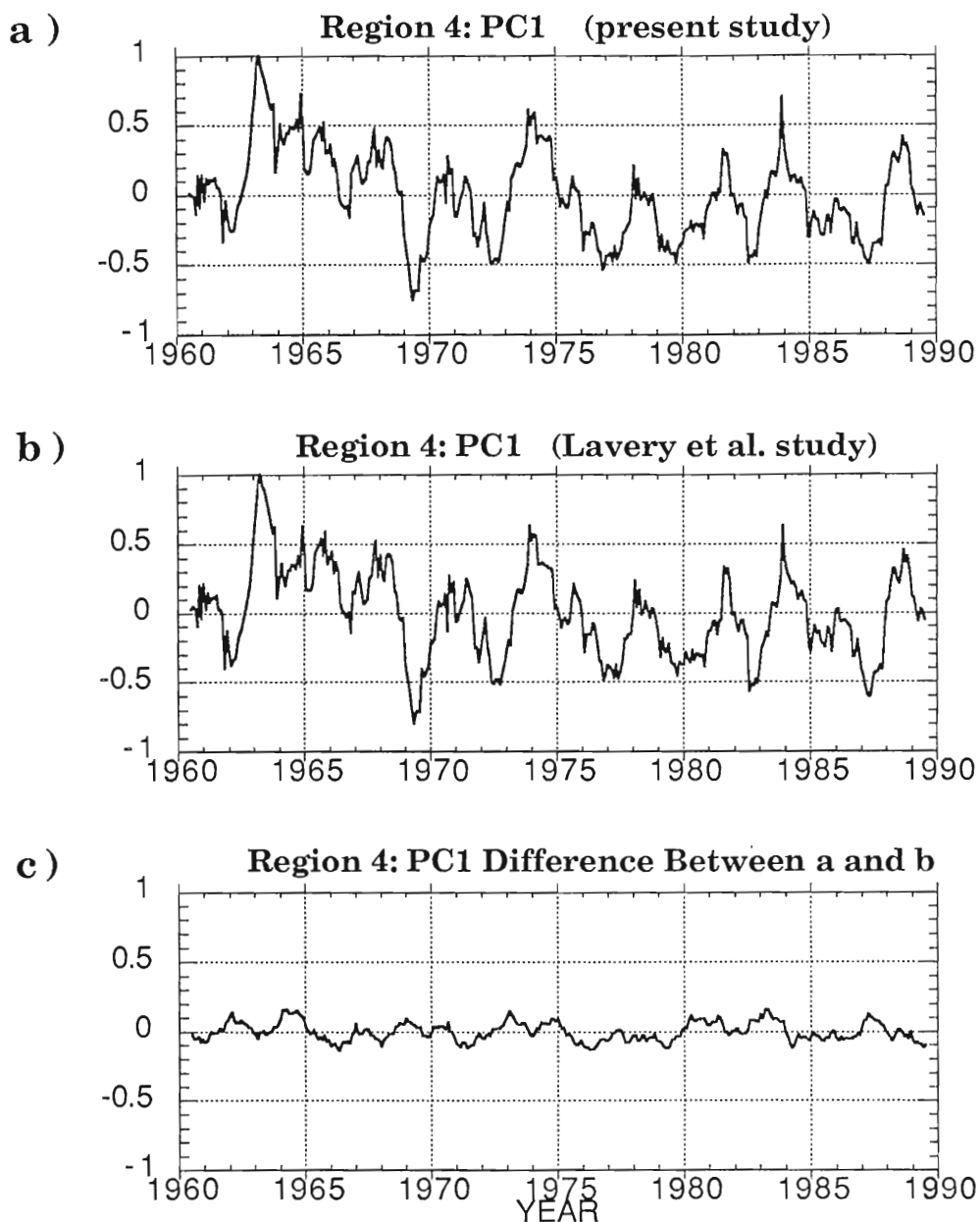


Fig. 1: a) First principal component (PC1) for Region4 (i.e. southwest Australia-see Fig. 3) of the present study. b) PC1 of the higher quality data set of Lavery et al. (1992) for the same region of interest. Each PC1 is normalized by the largest value within that time series. c) The difference between the two time series (a) and (b).

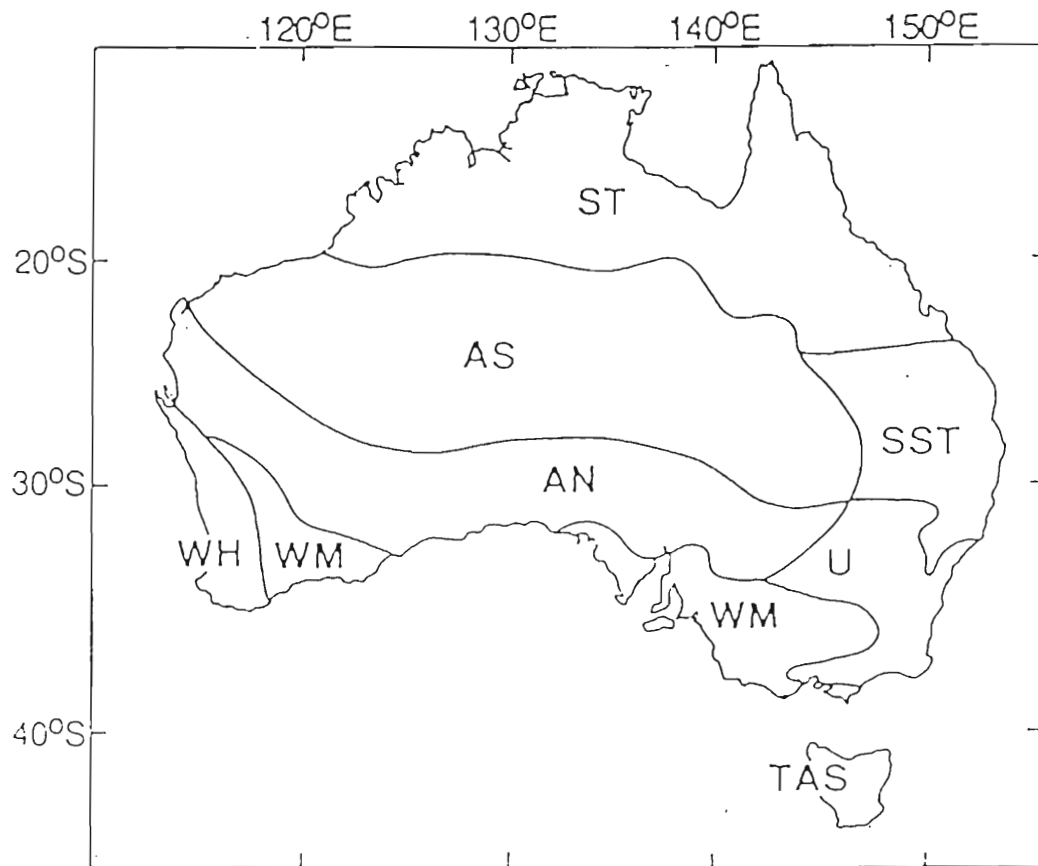


Fig. 2: Australian rainfall climate regions used by Srikanthan and Stewart (1991).



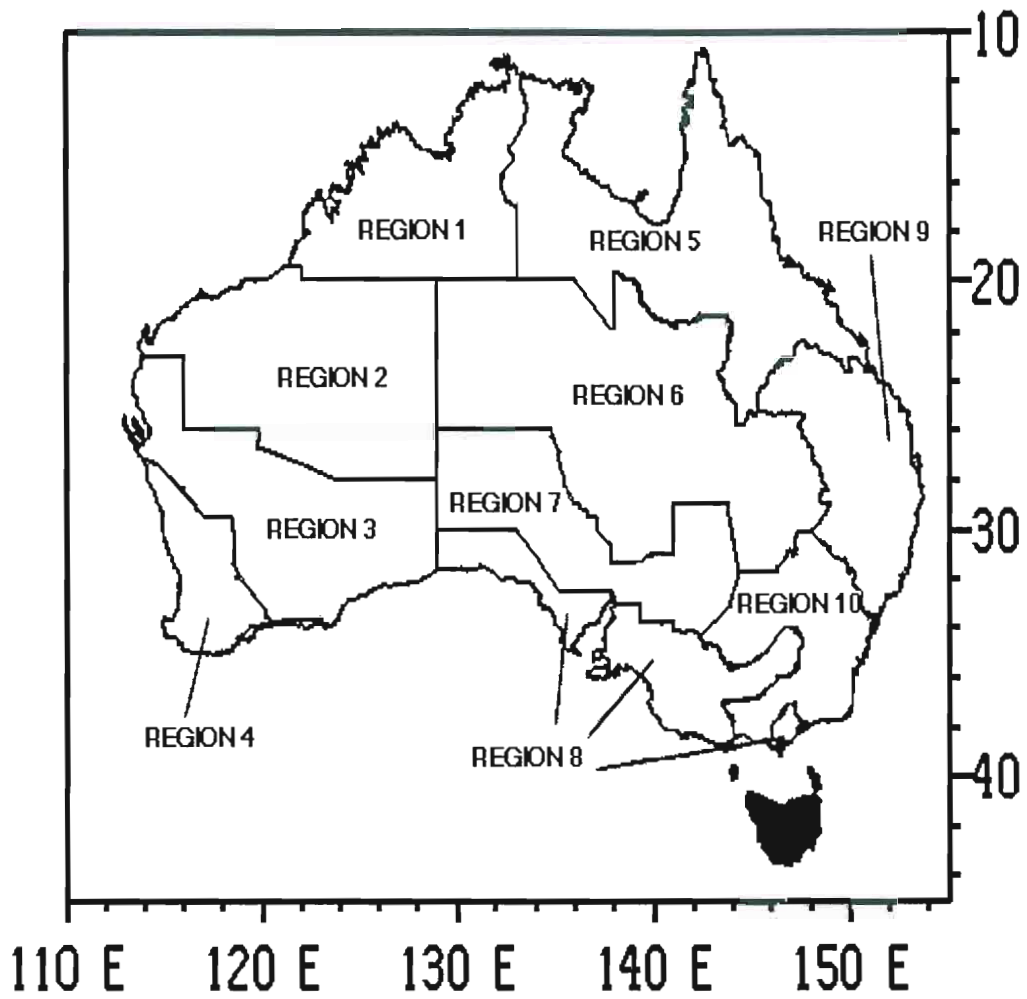
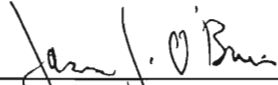


Fig. 3: Australian seasonal rainfall regions used in the present study.

The members of the Committee approve the thesis of Kenneth W.  
Ekers defended on November 29, 1994.



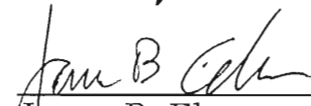
---

James J. O'Brien  
Professor Directing Thesis



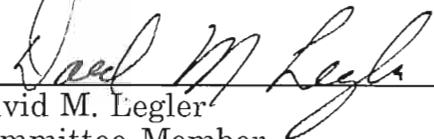
---

Eric A. Smith  
Committee Member



---

James B. Elsner  
Committee Member



---

David M. Legler  
Committee Member

To my wonderful wife, Heather, for all her love and support and to my  
parents for their encouragement to pursue my dreams.

## **Acknowledgement**

The basic support for the Center for Ocean-Atmospheric Prediction Studies is from the Secretary of Navy Chair to Dr. James J. O'Brien from the Physical Oceanography Program of the Office of Naval Research. My support was derived from the office of Global Programs, NOAA.

I wish to thank Dr. O'Brien, my major professor and thesis advisor, for his advice and instruction during my course of study at Florida State University. I also wish to express my gratitude to Dr. David M. Legler, thesis advisor and committee member, for his support and professional instruction. Additional thanks is offered to Dr. James B. Elsner, committee member, for his assistance in the area of statistics and to Paul T. Beaudoin and Matthew C. Sittel for their advice on scientific writing.

I wish to thank my wife for her love, encouragement and support. Thanks also to my colleagues at the Center for Ocean-Atmospheric Prediction Studies for their constructive comments and suggestions.

## Table of Contents

<b>List of Tables</b> .....	vii
<b>List of Figures</b> .....	viii
<b>Abstract</b> .....	x
<b>1. Introduction</b> .....	1
<b>2. Data</b> .....	5
2.1 Australian Rainfall Data Set.....	5
2.2 Latent Heat Flux (LHF) Data Set.....	9
2.3 Japan Meteorological Agency (JMA) Index.....	12
<b>3. Method</b> .....	14
3.1 Data Preparation.....	14
3.1.1 Rainfall.....	14
3.1.2 Latent Heat Flux.....	15
3.2 Empirical Orthogonal Function (EOF) Analysis for Rainfall and LHF.....	15
3.3 Rotation of Eigenvectors.....	16
<b>4. Results and Discussion</b> .....	19
4.1 Rainfall EOFs.....	19
4.2 Latent Heat Flux EOFs.....	41
4.3 Cross correlations.....	41
4.3.1 Relationship between LHF and JMA.....	42
4.3.1 Relationship between LHF and JMA.....	42
4.3.2 Relationship between Australian rainfall and LHF.....	42



4.3.3 Relationship between Australian rainfall and JMA index.....	49
5. Summary and Conclusions.....	55
Appendix A: EOF Analysis.....	58
Appendix B: Rotation of EOFs.....	61
References.....	64
Biographical Sketch.....	68

## List of Tables

<b>Table 1:</b> Rainfall and LHF regions EOF results. Each of the ten rainfall regions plus the LHF region is utilized in an EOF analysis. The resulting eigenvectors (EOFs) are tested for significance using a Monte Carlo test (see text for full explanation). The significant EOFs account for a cumulative percent of the variant structure of the data for the given region.....	17
<b>Table 2:</b> Maximum correlation coefficient (for lead/lag of $\pm 12$ months) between Australian rainfall (PC1) and Indian Ocean LHF (PC1). The lead/lag at which the correlation occurs is also noted. A (-) in the 'LEAD/LAG' column indicates LHF anomalies lead rainfall anomalies by that many months. An <u>underlined</u> correlation coefficient indicates it is significant at 95% confidence. Note there are no significant correlations in this table.....	44
<b>Table 3:</b> Same as in Table 2 except for Australian rainfall (PC1) and Indian Ocean LHF (PC2).....	45
<b>Table 4:</b> Same as in Table 2 except for Australian rainfall (PC2) and Indian Ocean LHF (PC1).....	46
<b>Table 5:</b> Same as in Table 2 except for Australian rainfall (PC2) and Indian Ocean LHF (PC2).....	47
<b>Table 6:</b> Maximum correlation coefficient (for lead/lag of $\pm 12$ months) between Australian rainfall (PC1) and the JMA index. The lead/lag at which the correlation occurs is also noted. A (-) in the 'LEAD/LAG' column indicates negative (positive) SST anomalies in the eastern equatorial Pacific Ocean lead positive (negative) rainfall anomalies by that many months. An <u>underlined</u> correlation coefficient indicates it is significant at 95% confidence. Note all but two regions show significance.....	50
<b>Table 7:</b> Same as in Table 7 except for Australian rainfall (PC2). Region 4 rainfall anomalies show the most impressive 95% confidence. Note all but two regions show significance.....	50
<b>Table 7:</b> Same as in Table 7 except for Australian rainfall (PC2). Region 4 rainfall anomalies show the most impressive relationship with the ENSO indicator.....	52

## List of Figures

<b>Figure 1:</b> A test to demonstrate the quality of data. a) First principal component (PC1) for Region4 of the present study. b) PC1 of the higher quality data set of Lavery et al. (1992) for the same region of interest. Each PC1 is normalized by the largest value within that time series. c) The difference between the two time series (a) and (b).....	7
<b>Figure 2:</b> Australian rainfall climate regions used by Srikanthan and Stewart (1991).....	8
<b>Figure 3:</b> Australian seasonal rainfall regions used in the present study.....	10
<b>Figure 4:</b> Geographical region of the Indian Ocean from which latent heat flux (LHF) (Jones et al., 1994) is used. The region covers an area from 30°E-120°E and 8°S-30°S.....	11
<b>Figure 5:</b> JMA index (thin solid line) and its 12 month running mean (dashed line). Thick solid lines at $\pm 0.5^{\circ}\text{C}$ indicate extreme ENSO thresholds (i.e. El Niño $\{+0.5^{\circ}\text{C}\}$ and El Viejo $\{-0.5^{\circ}\text{C}\}$ ). Note indications of strongest El Niños in 1972, 1982 and 1986/87.....	13
<b>Figure 6:</b> a) The first rotated spatial field (EOF1) of normalized station loadings for Region 1, and b) its associated time series (PC1) of rainfall anomalies in units of millimeters. c) Same as in (a) except for the second rotated spatial field (EOF2), and d) same as in (b) except for PC2.....	20
<b>Figure 7:</b> Same as in Figure 6 except for Region 2.....	22
<b>Figure 8:</b> Same as in Figure 6 except for Region 3.....	24
<b>Figure 9:</b> Same as in Figure 6 except for Region 4.....	26
<b>Figure 10:</b> Same as in Figure 6 except for Region 5.....	28
<b>Figure 9:</b> Same as in Figure 6 except for Region 4.....	26
<b>Figure 10:</b> Same as in Figure 6 except for Region 5.....	28
<b>Figure 11:</b> Same as in Figure 6 except for Region 6.....	29

<b>Figure 12:</b> Same as in Figure 6 except for Region 7.....	32
<b>Figure 13:</b> Same as in Figure 6 except for Region 8.....	33
<b>Figure 14:</b> Same as in Figure 6 except for Region 9.....	35
<b>Figure 15:</b> Same as in Figure 6 except for Region 10.....	37
<b>Figure 16:</b> a) The first rotated spatial field (EOF1) of normalized station loadings for the LHF region. b) Same as in (a) except for EOF2. The associated time series of EOF1 (PC1) and d) the associated time seires of EOF2. The PCs display LHF anomalies in units of watts per meter squared ( $W m^{-2}$ ).....	41

## ABSTRACT

This study examines the variability of the spatiotemporal structure evident in Australian monthly mean rainfall totals. The study employs a varimax-rotated empirical orthogonal function (EOF) analysis to each of ten Australian climatic regions over a 30 year period (1960 - 1989). The study applies a similar EOF analysis to the monthly Indian Ocean latent heat flux (LHF) fields for the same time period over a portion of the southern tropical/subtropical region of the Indian Ocean for intercomparative analyses. These analyses focus on the variability of the significant EOF modes associated with the Australian rainfall and their relationship to eastern equatorial Pacific sea-surface temperature (SST) anomalies and the Indian Ocean LHF.

The temporal variability associated with the significant rotated EOFs of Australian rainfall account for 78% - 91% of the total variance and highlight the presence of a quasi-biennial oscillation throughout most of the ten regions. The study indicates a link between the quasi-biennial periodicity and lower, regionally dependent frequencies of 3 to 7 years. The temporal variability evident in the significant rotated EOFs of the Indian Ocean LHF account for 74% of the total variance and demonstrate evidence of a quasi-biennial signal.

It is known from the work of Pittock (1975) that Australian rainfall is strongly influenced by ENSO. This study reveals the central regions

It is known from the work of Pittock (1975) that Australian rainfall is strongly influenced by ENSO. This study reveals the central regions have the strongest relationship to the ENSO index. The southern rainbelt